THE MAGNETOTHERMOPOWER OF ORGANIC SUPERCONDUCTOR $\kappa-(\mathrm{ET})_2\mathrm{Cu}(\mathrm{NCS})_2$: POSSIBLE CHARGE DENSITY WAVE SCENARIO

DANICA KRSTOVSKA[1,a], EUN SANG CHOI[2], EDEN STEVEN[2,3]

[1]Ss. Cyril and Methodius University, Faculty of Natural Sciences and Mathematics, Arhimedova 3, 1000 Skopje, Macedonia
Corresponding author[a]: danica@pmf.ukim.mk; krstovska@magnet.fsu.edu
[2]National High Magnetic Field Laboratory, Florida State University, Tallahassee, FL 32310, USA
[3]Emmerich Education Center, Jakarta, Indonesia

Received June 6, 2021

Abstract. The interlayer magnetothermopower of the organic superconductor $\kappa-(\mathrm{ET})_2\mathrm{Cu}(\mathrm{NCS})_2$ is studied at temperatures down to 0.5 K and fields up to 32 T. Analysis of the background magnetothermopower shows that at low temperatures it is negative and exhibits an upturn at higher field, producing a dip at a field close to the upper critical field B_{c2}. There are clear magnetothermopower quantum oscillations visible above 5 T. The obtained oscillation frequencies are in a good agreement with those previously reported on the magnetoresistance and magnetization quantum oscillations. According to our results, the magnetothermopower in $\kappa-(\mathrm{ET})_2\mathrm{Cu}(\mathrm{NCS})_2$ presents features which have already been detected in YBCO and other high-T_c cuprates indicating that some kind of a charge density wave order is also present in the normal state of $\kappa-(\mathrm{ET})_2\mathrm{Cu}(\mathrm{NCS})_2$. Most strikingly, our measurements show that there is another dip, again followed by an upturn, in the magnetothermopower of $\kappa-(\mathrm{ET})_2\mathrm{Cu}(\mathrm{NCS})_2$ occurring at much higher fields than B_{c2}, around the magnetic breakdown field of ~ 21 T that is not present in YBCO. We propose that the two induced successive phase transitions, consisting of two similarly ordered states each restricted to a finite magnetic field window are in fact charge density wave ordered states arising as a result of the layer-stacking mechanism in the interlayer direction. Our results support and advance some of the previous findings that the superconductivity in the organic superconductor $\kappa-(\mathrm{ET})_2\mathrm{Cu}(\mathrm{NCS})_2$ is mediated by a charge density wave order rather than antiferromagnetic fluctuation.

Key words: Organic superconductor, $\kappa-(\mathrm{ET})_2\mathrm{Cu}(\mathrm{NCS})_2$, magnetothermopower, charge density wave, layer-stacking.

1. INTRODUCTION

Thermoelectric effects provide an important information concerning the sign of the transport carriers and may be useful for the study of the relation between the anisotropy of the electronic bands and superconducting state. The investigation of magnetothermopower in quantized magnetic field might give useful insights for the structure of the energy spectrum and the scattering processes especially in the case of anisotropic materials. Advantages of magnetothermopower measurements include obtaining information about both the thermodynamic and transport properties of carriers. From the variety of anisotropic materials, the layered organic molecular crystals $\kappa-(\mathrm{ET})_2\mathrm{X}$ (where ET is bis-(ethylenedithia-tetrathiafulvalene) and X is an anion ($\mathrm{X} = \mathrm{I}_3$, $\mathrm{Cu[N(CN)_2]Br}$, $\mathrm{Cu(NCS)_2}$)) are particularly interesting because they are strongly correlated electron systems with similarities to the high-T_c cuprate superconductors including unconventional metallic properties, strong electron correlation effect and the superconductivity [1, 2]. The crystalline organic metal $\kappa-(\mathrm{ET})_2\mathrm{Cu(NCS)_2}$ was chosen for the magntothermopower experiments because its Fermi surface (FS) comprises a Q2D pocket and a pair of Q1D sheets and is very well characterized [3–5]. The salt $\kappa-(\mathrm{ET})_2\mathrm{Cu(NCS)_2}$ has a high superconducting transition temperature ($T_c = 10.4$ K [6]), and it is probably the most popular and best characterized material out of all the organic charge-transfer salts based on the ET molecule. At low temperatures below 1 K and magnetic field below the upper critical field B_{c2}, a quantum vortex liquid (QVL) is realized due to the large quantum fluctuation [7, 8] while above 1 K a thermal vortex liquid (TVL) is present. The vortex phase diagram of $\kappa-(\mathrm{ET})_2\mathrm{Cu(NCS)_2}$ in a magnetic field perpendicular to the Q2D conducting plane obtained from the magnetoresistance measurements is given in Ref. [9]. The Shubnikov-de Haas (SdH) and de Haas-van Alphen (dHvA) oscillations are studied experimentally in both the mixed and normal state of the Q2D organic superconductor $\kappa-(\mathrm{ET})_2\mathrm{Cu(NCS)_2}$ [10, 11]. Sasaki *et al.* have shown that below the upper critical field B_{c2} there is an additional damping of the SdH and dHvA oscillations amplitude with respect to the normal state one which is described within the standard Lifshitz-Kosevich formula [11]. In the quantum fluctuation region at lower temperature SdH effect shows stronger amplitude damping than that of the dHvA oscillations. This organic superconductor has a number of similarities with the high-T_c cuprate YBCO [2]. If the same conventions are used for the magnetic Brillouin zone as in the high-T_c cuprates with $d_{x^2-y^2}$ symmetry, it was shown that the superconducting gap symmetry of $\kappa-(\mathrm{ET})_2\mathrm{Cu(NCS)_2}$ is d_{xy} [12, 13]. In addition, the thermal conductivity and scan tunnelling spectroscopy measurements predicted that the superconducting paring symmetry in this organic superconductor is more like d_{xy} than $d_{x^2-y^2}$ [13, 14]. On the other hand, theoretical studies have suggested that superconductivity with d_{xy} symmetry is based on the charge density wave (CDW) and charge fluctuation scenario [15, 16].

Here we report the first magnetic field measurements of the longitudinal or interlayer magnetothermopower (Seebeck effect) in the Q2D organic superconductor $\kappa-(\mathrm{ET})_2\mathrm{Cu(NCS)_2}$ at temperatures down to 0.5 K and fields up to 32 T. We find a striking similarity with the magnetothermopower behaviour in YBCO; the new features that appear in magnetothermopower of $\kappa-(\mathrm{ET})_2\mathrm{Cu(NCS)_2}$ are similar to those observed in the Seebeck effect of YBCO. A field-induced first dip near the upper critical field and a second one right above the magnetic breakdown field followed by an upturn might be an evidence for a formation of a CDW state or charge fluctuation in a direction perpendicular to the layers. Moreover, we find that the magnetothermopower of $\kappa-(\mathrm{ET})_2\mathrm{Cu}(\mathrm{NCS})_2$ is also similar to the one measured in the organic conductor $\alpha-(\mathrm{ET})_2\mathrm{KHg}(\mathrm{SCN})_4$ whose low temperature state is known to be a CDW state formed as a result of the nesting instability of the q1D band [17]. We find that the interlayer effects, *i.e.*, the layer-stacking along the interlayer direction rather than the nesting instabilities might be the dominant mechanism in possible CDW scenario in organic superconductor $\kappa-(\mathrm{ET})_2\mathrm{Cu}(\mathrm{NCS})_2$. Our results advance previous findings on possible existence of a CDW state in this material and its correlation with the superconducting order.

2. EXPERIMENT

Single crystals of $\kappa-(\mathrm{ET})_2\mathrm{Cu}(\mathrm{NCS})_2$ were synthesized by the electrocrystallization technique. The data presented in this work were taken in a $^3\mathrm{He}$ system with field up to 32 T at the National High Magnetic Field Laboratory at Tallahassee. Magnetic field measurements of the interlayer magnetothermopower were carried out by applying sinusoidal heat current along the crystallographic axis a^* of the single crystal. The sample was mounted between two quartz blocks, which were heated by sinusoidal heating currents (with an oscillation frequency f_0) with a $\pi/2$ phase difference. A miniature heater was placed on top of the sample to establish a small temperature gradient along the a^*-axis. The corresponding temperature gradient (∇T) and the thermal electromotive force (emf) with $2f_0$ oscillation frequency were measured. Two pairs of Au wires were attached to the sample along the a^* axis on the opposite sides of the bc planes of the sample by carbon paste for both the interlayer magnetoresistance and magnetothermopower measurements. The temperature gradient ∇T, which was found to be nearly field independent, was set prior to each magnetic field sweep. The detail procedures of the magnetothermopower measurement method used in this work are given elsewhere [18]. For the measurements reported here, the magnetic field and thermal gradient were applied parallel to the a^* axis, *i.e.*, perpendicular to the Q2D conducting bc plane as shown in Fig. 1.

3. RESULTS AND DISCUSSION

We show in Fig. 2 the total interlayer magnetic thermopower signal of the organic superconductor $\kappa-(\mathrm{ET})_2\mathrm{Cu}(\mathrm{NCS})_2$, $S_a^*(B)$, measured at three different temperatures: $T = 0.5$, 0.9 and 1.4 K. The total magnetothermopower consists of two parts, the background thermopower which is sensitive to the FS topology, and an oscillatory component which is a manifestation of the Landau quantization on

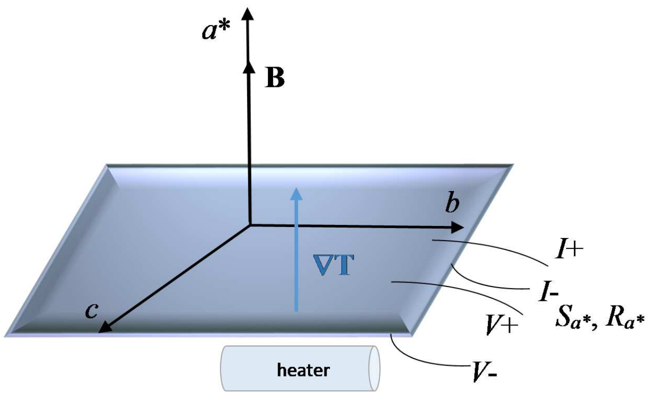

Fig. 1 – The experimental geometry for the interlayer magnetoresistance and thermopower (Seebeck effect) measurements in the organic superconductor $\kappa-(\mathrm{ET})_2\mathrm{Cu}(\mathrm{NCS})_2$ as a function of the magnetic field. The applied magnetic field and temperature gradient are along the less conducting axis a^* of the superconductor, perpendicular to the Q2D conducting bc plane.

the closed orbit of the FS. Figure 2 reveals complex behavior of the magnetothermopower of $\kappa-(\mathrm{ET})_2\mathrm{Cu}(\mathrm{NCS})_2$ which reflects its multiband character since two types of carriers are involved in the thermoelectric transport. As evident from Fig. 2, there is a prominent change in the thermopower character in $\kappa-(\mathrm{ET})_2\mathrm{Cu}(\mathrm{NCS})_2$ with increasing temperature and magnetic field as the system transitions from the QVL to TVL and to the normal state. As the magnetothermopower measurement is a sensitive probe of the density of states close to the FS the changes in the magnetothermopower are usually attributed to the change in the electronic band structure of the material. We first determine the irreversible magnetic field B_{irr} from the magnetothemopower measurements at each temperature. We define this field as the one at which the magnetothermpower of $\kappa-(\mathrm{ET})_2\mathrm{Cu}(\mathrm{NCS})_2$ goes to zero, *i.e.*, at witch the magnetothermpower changes sign from positive to negative. Thus, we find that B_{irr} is 3 T, 2.5 T and 1.5 T for 0.5 K, 0.9 K and 1.4 K, respectively. We obtain the same values for B_{irr} from our magnetoresistance measurements (Fig. 4 below) which are determined as the onset magnetic field of interlayer magnetoresistance R_{a*} and are in agreement with those previously obtained from the torque and magnetoresistance measurements [7, 11]. The superconducting state in $\kappa-(\mathrm{ET})_2\mathrm{Cu}(\mathrm{NCS})_2$, in the magnetic field perpendicular to the Q2D plane, develops below the field $B_{c2} \simeq 5$ T and temperature $T_c \sim 10$ K and consists of a vortex solid and two vortex liquid states. Indeed, according to the vortex phase diagram of $\kappa-(\mathrm{ET})_2\mathrm{Cu}(\mathrm{NCS})_2$, below B_{irr} the system is in the vortex solid state (VS) and in the region $B_{\mathrm{irr}} < B < B_{c2}$ there exist QVL or TVL state, depending on the temperature [9]. The QVL state is expected below 1 K with a weak non-linear behavior of the resistivity which is not observed in the TVL region above 1 K.

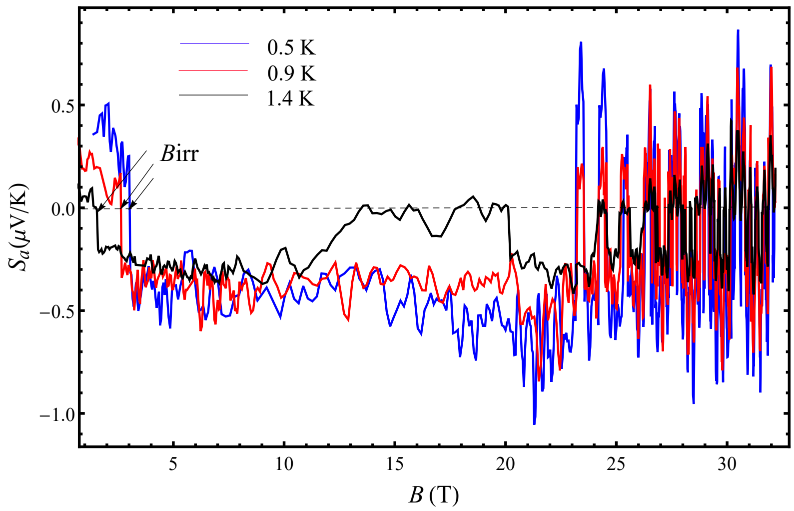

Fig. 2 – The total interlayer magnetothermopower of the organic superconductor $\kappa-(\mathrm{ET})_2\mathrm{Cu}(\mathrm{NCS})_2$, $S_a^*(B)$, measured in a magnetic field up to 32 T perpendicular to the conductive bc plane at three different temperatures: $T = 0.5$ K, 0.9 K and 1.4 K. The change in the magnetothermopower character is evident with increasing temperature and magnetic field.

As evident from Fig. 2, the magnetothermopower does not vanish, *i.e.*, it is not zero in the superconducting state as expected but instead is finite below the B_{c2}. This is consistent with previously reported finite magnetoresistance in the vortex liquid state of this compound [11]. Bellow B_{irr}, in the VS state, the magnetothermopower is positive and decreasing with increasing field up to the B_{irr}, reaching zero value at B_{irr}. In the region $B_{\mathrm{irr}} < B < B_{c2}$ and temperatures below 1 K, in the QVL state, the magnetothermopower has similar values whereas at temperature above 1 K and the same field region, in the TVL state, the magnetothermopower has lower values and is predominantly negative. In the normal state, above B_{c2}, the magnetothermopower of $\kappa-(\mathrm{ET})_2\mathrm{Cu}(\mathrm{NCS})_2$ is predominantly negative and there is a prominent change in the behavior with increasing field and temperature, *i.e.*, in the normal state. Indeed, Fig. 2 reveals a development of a pronounced feature in a form of an upturn above 15 T preceded by a dip at a magnetic field $B_S \sim 7$ T close to the upper critical field B_{c2}. With further increasing magnetic field the magnetothermopower slightly decreases and fast thermopower quantum oscillations emerge above 23 T. Interestingly, the appearance of a specific feature in a form of a dip followed by an upturn in the magnetothermopower of $\kappa-(\mathrm{ET})_2\mathrm{Cu}(\mathrm{NCS})_2$ is a behavior reminiscent to the one of the Seebeck coefficient in the orthorhombic high-T_c cuprate YBCO [19].

Moreover, our results show more complex behavior of the magnetothermopower of $\kappa-(\mathrm{ET})_2\mathrm{Cu}(\mathrm{NCS})_2$ compared to that observed in YBCO. Most strikingly, there is another upturn in the magnetothermopower of $\kappa-(\mathrm{ET})_2\mathrm{Cu}(\mathrm{NCS})_2$ at high magnetic fields followed by another dip at each temperature more pronounced than the lower field one. The new features observed in the organic superconductor κ−(ET)$_2$ Cu(NCS)$_2$ are more clearly visible in the magnetic field dependence of the interlayer background thermopower, $S_{a^*}^{\mathrm{bac}}(B)$, shown in Fig. 3. We see that at low temperatures there appear successive upturns at a certain field that produce dips near the upper critical field B_{c2} and again around the magnetic breakdown field $B_{\mathrm{MB}} \sim 20$ T, respectively.

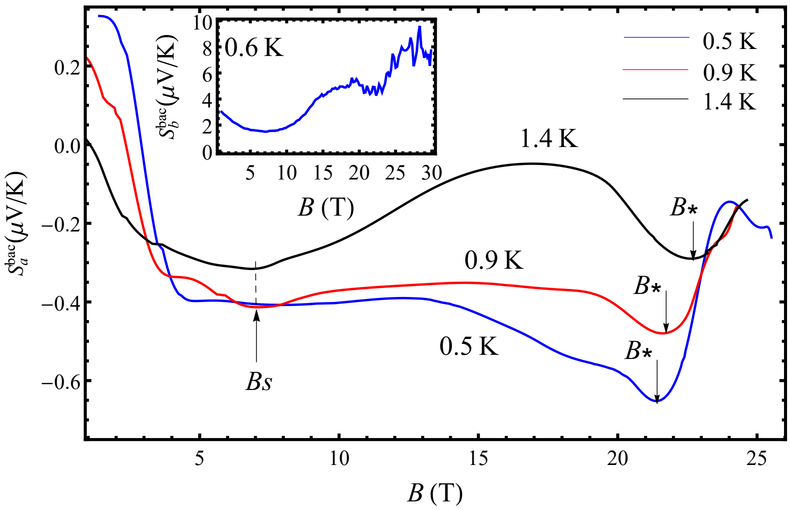

Fig. 3 – Magnetic field dependence of the background interlayer thermopower in $\kappa-(\mathrm{ET})_2\mathrm{Cu}(\mathrm{NCS})_2$ at 0.5, 0.9 and 1.4 K. The onset fields B_S and B^* for CDW order are indicated for reference. The inset shows the interlayer thermopower of the organic conductor $\alpha-(\mathrm{ET})_2\mathrm{KHg}(\mathrm{SCN})_4$ at low temperature of 0.6 K.

The first dip in the magnetothermopower is seen at a field $B_S \sim 7$ T, slightly above the upper critical field B_{c2}, followed by an upturn at $B = 17$ T for $T = 1.4$ K. This feature is not observed in the magnetothermopower at $T = 0.5$ K but it starts to develop at $T = 0.9$ K. Obviously, it becomes more pronounced and broaden with increasing temperature above 1 K in the normal state of $\kappa-(\mathrm{ET})_2\mathrm{Cu}(\mathrm{NCS})_2$. The second dip emerges at fields around the magnetic breakdown field $B^* \sim B_{\mathrm{MB}} \sim 21-22$ T and is well pronounced at each temperature. This results in appearance of another upturn in the magnetothermopower around $B \sim 24-26$ T depending on the temperature.

The negative magnetothermopower and the observed new features might be indicative of a change in the electronic configuration in this organic superconductor, *i.e.*, it might signify a presence of a FS reconstruction in $\kappa-(\mathrm{ET})_2\mathrm{Cu}(\mathrm{NCS})_2$ at low temperatures similarly as detected in YBCO. The changes in the magnetothermopower are usually attributed to the change of the electronic band structure, associated with the change in the electron-hole asymmetry due to a transition of the system into another ordered state. Given the striking similarity in the transport properties of YBCO and $\kappa-(\mathrm{ET})_2\mathrm{Cu}(\mathrm{NCS})_2$, the observed dips in the magnetothermopower of $\kappa-(\mathrm{ET})_2\mathrm{Cu}(\mathrm{NCS})_2$ may also be due to the development of a charge density wave order or charge fluctuation. In that context, a negative thermopower signifies presence of a small electron pocket caused by FS reconstruction related to CDW modulations. As in $\kappa-(\mathrm{ET})_2\mathrm{Cu}(\mathrm{NCS})_2$ the onset magnetic field B_S for CDW is slightly above the upper critical field it follows that the CDW order should emerge in the normal state of the material. However, in $\kappa-(\mathrm{ET})_2\mathrm{Cu}(\mathrm{NCS})_2$ the emergence of the CDW might be more intriguing than in YBCO as it appears to be correlated with the occurrence of the superconductivity and the magnetic breakdown simultaneously. Our results support the idea that the CDW order or charge fluctuation, and not the antiferromagnetic spin fluctuation, could be the origin of the superconductivity in $\kappa-(\mathrm{ET})_2\mathrm{Cu}(\mathrm{NCS})_2$ in accordance with previously proposed in a number of papers. Indeed, Sasaki *et al.* [20] on the base of the magnetic susceptibility measurements have found that in the organic superconductor $\kappa-(\mathrm{ET})_2\mathrm{Cu}(\mathrm{NCS})_2$ a CDW order or charge fluctuation coexists with the metallic (normal) phase between T_c and $T^* = 46-50$ K. They have proposed a possible CDW instability on the open part of FS. For $\kappa-(\mathrm{ET})_2\mathrm{Cu}(\mathrm{NCS})_2$, the b direction is expected to be a good nesting direction for the Q1D part of FS. However, our results indicate that a possible CDW order may develop along the a^*, *i.e.*, in the direction perpendicular to the Q1D part of FS where no nesting instability is expected. Additionally, thermal conductivity [13] and scan tunnelling spectroscopy [14] measurements also predicted that in $\kappa-(\mathrm{ET})_2\mathrm{Cu}(\mathrm{NCS})_2$ the superconducting paring symmetry is more like d_{xy} and superconductivity with d_{xy} symmetry has been theoretically suggested to be due to CDW order [15, 16]. If the nesting instability is the leading mechanism for the CDW order than one possibility is that in $\kappa-(\mathrm{ET})_2\mathrm{Cu}(\mathrm{NCS})_2$ there is a bidirectional CDW, similar to the one observed in YBCO [19], due to some structural changes occurring along the b direction. This, however, is not unexpected as in a multiband system such as $\kappa-(\mathrm{ET})_2\mathrm{Cu}(\mathrm{NCS})_2$ the total magnetothermopower may involve a mixing of contributions from several FS sections leading to magnetic breakdown. Another possibility is that experimentally, there is always a possibility of random diffusion of heat in the sample due to a misalignment between the heat current and the crystallographic axis. In that case, the in-plane or transverse magnetothermopower components could be significant and their mixing can in general affect the overall behavior of the interlayer magnetothermopower. Our results also indicate that the possible CDW order in $\kappa-(\mathrm{ET})_2\mathrm{Cu}(\mathrm{NCS})_2$ should exist not only between T_c and

T^* but down to $T \sim 1$ K as the dip in the magnetothermopower develops above 1 K for the direction perpendicular to the conducting plane. This indicates that if indeed a CDW phase is formed than the superconductivity in the organic superconductor $\kappa-(\mathrm{ET})_2\mathrm{Cu(NCS)}_2$ should be considered on the basis of this phase. Furthermore, we find that the magnetothermopower of $\kappa-(\mathrm{ET})_2\mathrm{Cu(NCS)}_2$ does not go to zero in the superconducting state (except at B_{irr}) as observed in YBCO, suggesting a possibility of coexistence of both the superconducting and CDW order. With decreasing magnetic field below the onset field for the first dip, B_S, the thermopower increases instead of vanishing which indicates that in $\kappa-(\mathrm{ET})_2\mathrm{Cu(NCS)}_2$ the possible CDW order would not be totally suppressed by the superconductivity as it is case in YBCO. However, unlike the compelling evidence that the FS reconstruction in YBCO is caused by CDW modulations as observed by X-ray diffraction (XRD) there is not such evidence for $\kappa-(\mathrm{ET})_2\mathrm{Cu(NCS)}_2$.

For the purpose of this work we have also measured the magnetothermopower of the organic conductor $\alpha-(\mathrm{ET})_2\mathrm{KHg(SCN)}_4$ whose low temperature ground state is a CDW state associated with the nesting instability of the q1D band. The background magnetothermopower of $\alpha-(\mathrm{ET})_2\mathrm{KHg(SCN)}_4$ at $T = 0.6$ K is shown in the inset of Fig. 3. We find a striking similarity between the background magnetothermopower behavior of both compounds only that the magnetothermopower of $\alpha-(\mathrm{ET})_2\mathrm{KHg(SCN)}_4$ is positive in the whole magnetic field range, which is a signature of a closed hole pocket on the FS. Apart from that, the same trend in a form of a dip and an upturn is also apparent with increasing field up to temperatures of $T = 4$ K [21, 22] as in $\kappa-(\mathrm{ET})_2\mathrm{Cu(NCS)}_2$. However, in $\kappa-(\mathrm{ET})_2\mathrm{Cu(NCS)}_2$ the whole picture based on CDW scenario is more intriguing as the probability for FS nesting is small and possible only along $b-$axis. This indicates that another mechanism should be involved in the emergence of CDW modulations in this material.

In order to further obtain insights into the development of possible CDW order in $\kappa-(\mathrm{ET})_2\mathrm{Cu(NCS)}_2$ we have also measured the interlayer magnetoresistance at the same temperatures shown in Fig. 4. Following the Boltzmann transport theory a similarity between the magnetoresistance and magnetothermopower should be expected as the thermopower tensor S is a product of the resistivity tensor ρ and the thermoelectric tensor α, $S = \rho\alpha$, with the thermoelectric tensor expressed by the Mott formula $\alpha_{ij} = \frac{\pi^2 k_B T}{3e} \frac{d\sigma_{ij}(\varepsilon)}{d\varepsilon} |_{\varepsilon=\mu}$, where μ is the chemical potential of the electron system and $\sigma(\varepsilon)$ is the energy-dependent electrical conductivity.

Figure 4 shows that the interlayer magnetoresistance, $R_a^*(B)$, also undergoes a prominent change with increasing temperature and field. Over certain ranges of temperature and magnetic field there appears an anomalous resistance maximum or a 'hump' in the magnetoresistance of $\kappa-(\mathrm{ET})_2\mathrm{Cu(NCS)}_2$ between the superconducting and normal state. This is in agreement with previous magnetoresistance studies

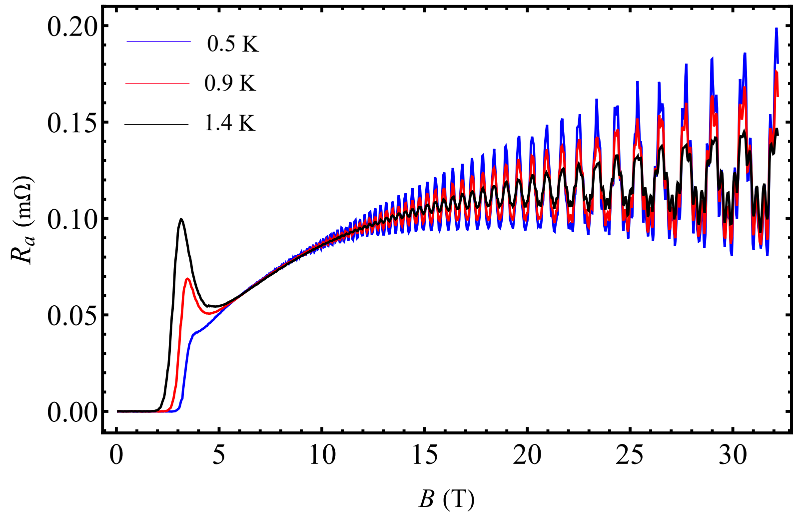

Fig. 4 – The interlayer magnetoresistance of $\kappa-(\mathrm{ET})_2\mathrm{Cu(NCS)}_2$, $R_a^*(B)$, measured in magnetic field up to 32 T and three different temperatures: $T = 0.5$ K, 0.9 K and 1.4 K. The SdH oscillations and the presence of the 'hump' are clearly visible.

in this material. The 'hump' anomaly has been reported only for the interlayer resistivity, but not in the in-plane resistivity, and its existence has been attributed to the several factors [23–27]. As seen from Fig. 4 the height of the resistance maximum changes and shifts to lower fields with increasing temperature. In comparison, we find that the first dip in the magnetothermopower, observed near the upper critical field, starts to develop around the magnetic field where the 'hump' in the magnetoresistance occurs. The anomalous 'hump' becomes more prominent with increasing temperature, especially above 1 K, (it exists up to the transition temperature $T_c \sim 10$ K) in accordance with previous reports [9]. Interestingly, the magnetothermopower follows the similar trend in its magnetic field behavior characterized with an appearance of a dip that develops near the magnetic field where the 'hump' in the magnetoresistance occurs which is also more pronounced with increasing temperature above 1 K, in the TVL state. The magnetoresistance 'hump' and the magnetothermopower dip are still visible at $T = 0.9$ K although significantly reduced. As the 'hump' is present in the TVL state, this might indicate that in our sample the transition from the QVL to TVL state starts around $T = 0.9$ K. Although there have been many attempts to explain the origin of the magnetoresistance maximum in $\kappa-(\mathrm{ET})_2\mathrm{Cu(NCS)}_2$ a reasonable explanation has not been given yet. Hence, our findings make an additional contribution to these attempts in order to establish the origin for the unconventional superconductivity in this system. Following the magnetothermopower behavior we propose that the existence of the magnetoresistance 'hump' might be correlated with the presence of a CDW order that develops in the normal state of $\kappa-(\mathrm{ET})_2\mathrm{Cu(NCS)}_2$ and is not totally suppressed in the vortex state. Interestingly, the in-plane thermal conductivity of $\kappa-(\mathrm{ET})_2\mathrm{Cu(NCS)}_2$ [13], in a field perpendicular to the conducting plane, also exhibits a dip at a magnetic field that corresponds to the one of the magnetoresistance 'hump'. However, while the magnetoresistance 'hump' and the thermal conductivity dip appear slightly below the upper critical field, around $3-3.5$ T depending on the temperature, the magnetothermopower dip occurs at magnetic field slightly above the the upper critical field, around 7 T, and is temperature independent. Considering the fact that on the one hand, the possibility for nesting along the interlayer direction is almost non-existent and that on the other hand, the magnetoresistance, thermal conductivity and magnetothermopower reveal existence of features essentially present when the magnetic field is perpendicular to the conducting layers, our observations imply that the existence of possible CDW modulations as a primary cause for the observed features can be attributed not to the nesting instability on the Q1D part of FS (at least not totally to that mechanism) but rather to the interlayer effects in this material.

With the appearance of the second magnetothermopower dip around $B^* \sim B_{MB} \sim 21-22$ T, there is a possibility that the system undergoes a second density wave instability along the a^*-axis. In that case, in $\kappa-(\mathrm{ET})_2\mathrm{Cu(NCS)}_2$, a cascade of density wave transitions might occur. The high field state may be realized by the same mechanism as the low field one or it could be correlated with the magnetic breakdown and the formation of new small orbits observed in the normal state only in the magnetothermopower and not in the magnetoresistance. Any new oscillations allowed with the magnetic breakdown will depend on the strength of the CDW order. It is important to note that the magnetic field at which the second dip in the magnetothermopower of $\kappa-(\mathrm{ET})_2\mathrm{Cu(NCS)}_2$ appears also coincides with the upper critical magnetic field ($B_{c2} \sim 21$ T) at witch the system undergoes a phase transition from the superconducting mixed state into a Fulde-Ferrell-Larkin-Ovchinnikov (FFLO) state for magnetic fields applied parallel to the 2D superconducting layers [28]. It is known that a FS prone to nesting, but not sufficient to induce a density wave state, is one of the necessary conditions for inducing a FFLO state which for $\kappa-(\mathrm{ET})_2\mathrm{Cu(NCS)}_2$ is achieved according to the measured FS topology [29, 30]. This is further indication that nesting instabilities are not the primary cause for the formation of a CDW state in $\kappa-(\mathrm{ET})_2\mathrm{Cu(NCS)}_2$ even when the magnetic field lies precisely in the quasi-two-dimensional planes, specifically along the b–axis which is the nesting direction in this organic superconductor.

In order to obtain more information about the cause for a possible new ordered state in $\kappa-(\mathrm{ET})_2\mathrm{Cu(NCS)}_2$, we further analyze the magnetothermopower quantum oscillations shown in Fig. 5 at $T = 0.5$, 0.9 and 1.4 K. The magnetothermopower oscillations are visible above 5 T.

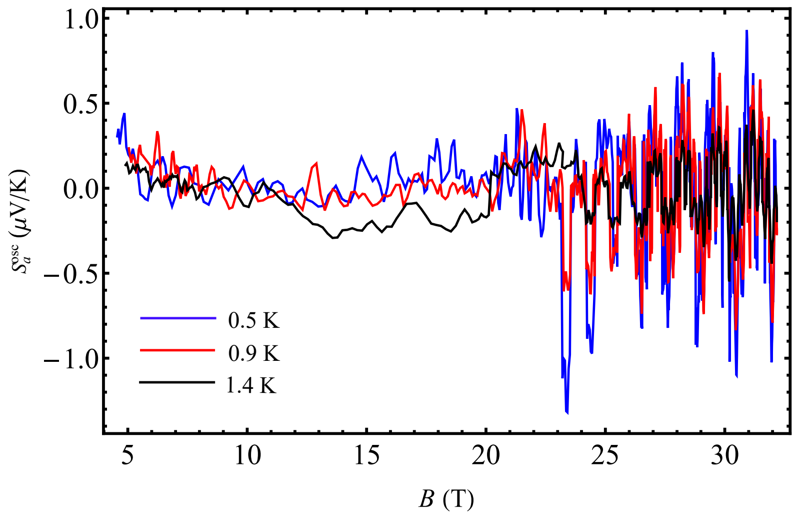

Fig. 5 – The interlayer magnetothermopower quantum oscillations obtained by filtering out the background signal from the total magnetothermopower at the same temperatures as in Fig. 2. At lower fields the magnetothermopower quantum oscillations are due to the α and 2α frequencies whereas fast magnetothermopower quantum oscillations due to the breakdown β orbit and the combination frequencies are seen at high fields above $B_{\rm MB} \sim 21$ T.

At lower fields the oscillations are due to the fundamental α frequency and it second harmonic whereas fast magnetothermopower quantum oscillations due to the breakdown β orbit and the combination orbits are seen at high fields above the magnetic breakdown field $B_{\rm MB} = 21$ T. The obtained low field magnetothermopower frequencies of $F_\alpha \sim 600$ T and $F_\beta \sim 3290$ T are in a good agreement with previous reports on the SdH and dHvA oscillations [10, 29]. The FFT spectrum of magnetoresistance in a given magnetic field range shown in Fig. 6a reveals existence of several frequencies while there is a plethora of frequencies in the FFT spectrum of magnetothermopower shown in Fig. 6b. The first two peaks in the low frequency region are due to the fundamental oscillations, F_α and its heavily damped (especially at $T = 1.4$ K) second harmonic $F_{2\alpha}$. Interestingly, $F_{3\alpha}$ frequency is present in Fig. 6a only at $T = 0.5$ K while in Fig. 6b only at $T = 1.4$ K.

In the high frequency region, three peaks are clearly seen at 0.5 K in the magnetoresistance FFT spectrum while there are more combination frequencies in the magnetothermopower FFT spectrum and some of the frequencies present in the latter are absent in the former. Usually in the FFT spectrum, there appear many extra peaks with the combination frequencies. The motion of the electrons (holes) in a magnetic field when the magnetic breakdown occurs makes several paths through some magnetic breakdown junctions. The presence of F_β, forbidden $F_\beta - F_\alpha$ and $F_\beta - F_{3\alpha}$ frequencies as well as permitted $F_\beta + F_\alpha$ frequency are visible in the

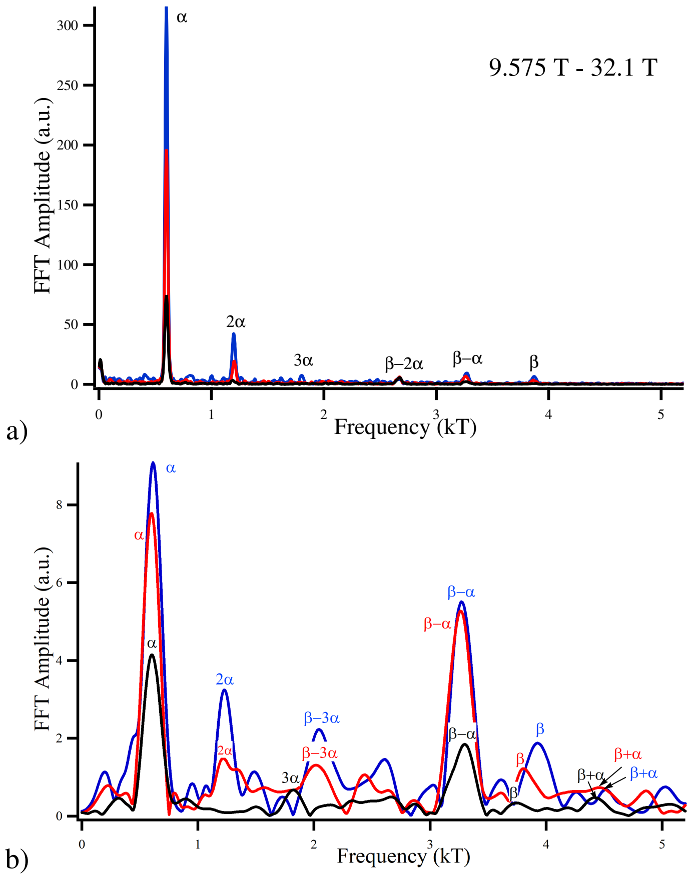

Fig. 6 – FFT spectrum of the a) magnetoresistance and b) magnetothermopower in a given magnetic field range with a plethora of frequencies.

magnetothermopower FFT spectrum. Apart from that, FFT spectrum of magnetoresistance reveals existence of F_β and another forbidden frequency $F_\beta - F_{2\alpha}$ in addition to $F_\beta - F_\alpha$ while $F_\beta + F_\alpha$ frequency is absent. The existence of forbidden frequencies was explained within the coherent magnetic breakdown model for a two-dimensional Fermi surface consisting of two open sheets and closed pockets connected by magnetic breakdown centers [10]. An important aspect of our measurements is that the forbidden by standard theories for magnetic breakdown $F_\beta - F_\alpha$ frequency is the dominant high-frequency oscillation (not F_β frequency) in the magnetothermopower of $\kappa-(\mathrm{ET})_2\mathrm{Cu}(\mathrm{NCS})_2$. The dominant presence of the $F_\beta - F_\alpha$ frequency was first reported only in the magnetoresistance and later also in the magnetization of $\kappa-(\mathrm{ET})_2\mathrm{Cu}(\mathrm{NCS})_2$ suggesting that there is more than one mechanism contributing to its existence. The strong presence of this frequency in the magnetothermopower, as obtained from our measurements, is however, expected as the magnetothermopower reflects both thermodynamic and transport properties of charge carriers. Harrison *et al.* [29] have shown that that a significant presence of this frequency can be explained not only by taking into account the oscillations of the chemical potential at high magnetic fields but also to the Stark quantum interference effect.

Sasaki *et al.* [20] have shown that in $\kappa-(\mathrm{ET})_2\mathrm{Cu(NCS)}_2$, below the upper critical field B_{c2}, there is an additional amplitude damping in the vortex state of the SdH and dHvA oscillation amplitude with respect to the normal state which is described with the standard Lifshitz-Kosevich (LK) formula by adding an additional damping term in the vortex state R_{SC} [31–33]. An important result of our measurements arises from analyzing the amplitude of quantum oscillations of both magnetoresistance and magnetothermopower in the normal state of $\kappa-(\mathrm{ET})_2\mathrm{Cu(NCS)}_2$. Indeed, our analysis shows that there is a damping of the oscillation amplitude in the normal state below $B\sim 10$ T and above $T=1$ K which is seen in the magnetothermopower but not in the magnetoresistance. We apply the LK formula to fit our experimental data. The amplitude A_{LK} of the first harmonic of the oscillations in the single band is given by $A_{\mathrm{LK}}^{\mathrm{MR}}\sim B^{1/2}R_TR_DR_S$ for magnetoresistance and $A_{\mathrm{LK}}^{\mathrm{MTEP}}\sim B^{-1/2}R_TR_DR_S$ for magnetothermopower where $R_T=(14.69m^*T/B)/\sinh(14.69m^*T/B)$ is the temperature factor, $R_D=\exp(-m_bT_D/B)$ is the Dingle factor, $R_S=\cos(gm_b/2m_e)$ is the spin factor. Here m^* is the effective electron mass, m_b is the band mass, m_e is the free electron mass and g is the conduction electron $g-$factor. Figures 7a and 7b show that at low temperature, $T=0.5$ K, there is no amplitude change either for the magnetoresistance or for the magnetothermopower in the normal state and both oscillation amplitudes are well described by the standard LK formula. However, with increasing temperature there is a significant change in the magnetothermopower oscillation amplitude below 10 T. Figure 7c shows that the magnetoresistance oscillation amplitude does not undergo damping at any magnetic field at $T=1.4$ K and again is well described by the LK formula but that is not the case with the amplitude of the magnetothermopower which at $T=1.4$ K starts to deviate from the LK behavior below 10 T as seen from Fig. 7d.

It is interesting to note that the first dip in the magnetothermopower starts to develop around this field with decreasing field (Fig. 3) and as we have associated the appearance of the dip with a possible CDW order this would indicate that the damping of the magnetothermopower oscillation amplitude might be correlated with the existence of some kind of CDW order in $\kappa-(\mathrm{ET})_2\mathrm{Cu(NCS)}_2$. It was shown that the SdH and dHvA oscillations in cuprates also deviate from the LK theory and the mechanisms of these deviations are in part the same as in layered organic superconductors. According to Gvozdikov [34], a typical mistake is an application of the thermodynamic set of the damping factors to the kinetic SdH oscillations.

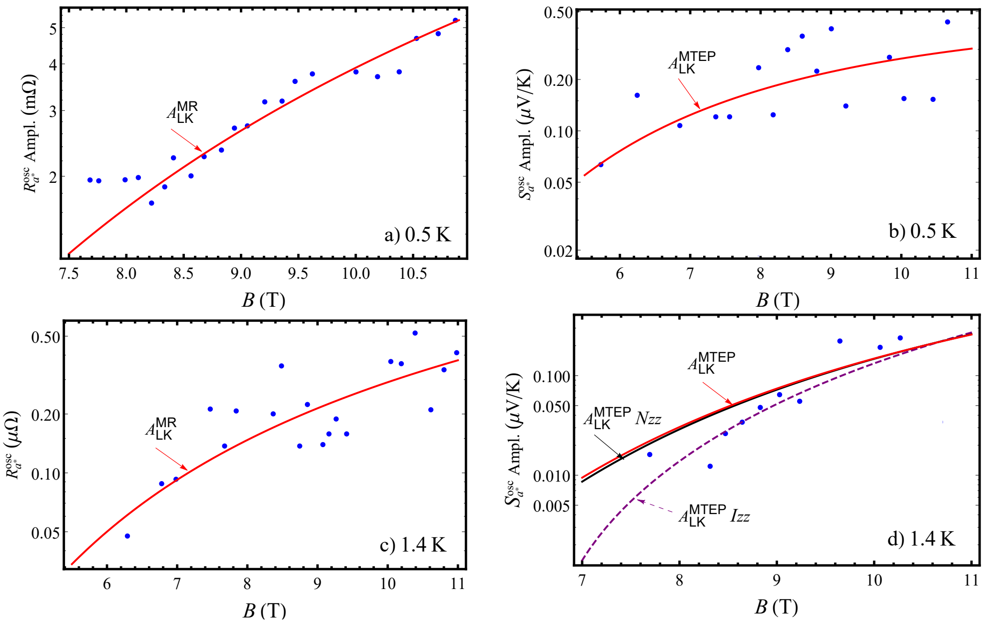

Fig. 7 – (Color online). Magnetic field dependence of the oscillation amplitude of a) interlayer magnetoresistance at 0.5 K, b) interlayer magnetothermopower at 0.5 K, c) interlayer magnetoresistance at 1.4 K and d) interlayer magnetothermopower at 1.4 K. The blue symbols are the experimental data, solid red curves are the field dependence of the oscillation amplitude based on the standard LK formula. The black and purple curves are the field dependence of the magnetothermopower oscillation amplitude with multiplying the LK formula with the kinetic and thermodynamic layer-stacking factors, N_{zz} and I_{zz}, respectively. The fitting is obtained using the following values: effective mass $m^* = 3.8m_e$ at 0.5 K and $m^* = 3.5m_e$ at 1.4 K, band mass $m_b = 1.2m_e$, $g = 1.8$ and Dingle temperature $T_D = 0.27$ K.

Following this, in order to further investigate the observed magnetothermopower behavior above $T = 1$ K and below $B \sim 10$ T, in the normal state of $\kappa-(\mathrm{ET})_2\mathrm{Cu}(NCS)_2$, we take into account the layer-stacking factors to fit the magnetothermopower amplitude in Fig. 7d that are not entering the standard LK formula and are different for the thermodynamic (dHvA) and kinetic (SdH) oscillations. These factors arise from the broadening of Landau levels into the bands due to electron hopping across the layers. For a periodic layer stacking and under the condition of a nearest layer electron hopping they are expressed in terms of the Bessel functions [34–37]. In Fig. 7, the solid red curve is the magnetothermopower oscillation amplitude obtained by the LK formula, $A_{\mathrm{LK}}^{\mathrm{MTEP}}$. The black solid curve in Fig. 7d is fitting of the magnetothermopower amplitude, $A_{\mathrm{LK}}^{\mathrm{MTEP}} N_{zz}$, by taking into account the kinetic layer-stacking factor for coherent electron motion across the layers $N_{zz} = 0.1BJ_1(2\pi t/\hbar\omega_c)$ (t is the interlayer hopping integral, $\omega_c = eB/m^*$ is the cyclotron frequency and J_1 is Bessel function of the first kind of order one), which is responsible for the SdH amplitude and oscillates in inverse magnetic field due to the warping of the FS. The purple solid curve in Fig. 7d is fitting of the magnetothermopower amplitude, $A_{\mathrm{LK}}^{\mathrm{MTEP}} I_{zz}$, by taking into account the oscillating thermodynamic layer-stacking factor $I_{zz} = J_0(4\pi t/\hbar\omega_c)$ (J_0 is Bessel function of the first kind of order zero) which is an oscillating function of the inverse magnetic field that modulates the dHvA oscillations. We obtain a good fitting of the magnetothermopower oscillation amplitude below 10 T with taking into account the thermodynamic layer-stacking factor I_{zz} under assumption that electrons scatter only within the layers and the interlayer hopping is independent of scattering whereas the inclusion of the kinetic layer-stacking factor N_{zz} describes a behavior very similar to that obtained by the LK formula as seen from Fig. 7d. It follows that, in $\kappa-(\mathrm{ET})_2\mathrm{Cu}(\mathrm{NCS})_2$, although magnetothermopower yields information about both thermodynamic and transport properties of charge carriers, the magnetothermopower quantum oscillations are thermodynamic in nature. This further confirms above discussed that the interlayer effects and not the nesting are important in the formation and existence of a possible CDW order as a predecessor of the superconducting state in this organic superconductor. The mechanism of layer-stacking in the interlayer direction might has a profound effect on the lattice parameters of the material leading to certain structural changes in this direction. Moreover, superconductivity and magnetic breakdown also modulate the factor I_{zz}. Considering that the onset fields in the magnetothermopower of $\kappa-(\mathrm{ET})_2\mathrm{Cu}(\mathrm{NCS})_2$ for CDW, B_S and B^*, are close to the upper critical field and the magnetic breakdown field and that the magnetothermopower oscillation amplitude is well fitted by taking into account the thermodynamic stacking factor I_{zz} below $B \sim 10$ T is a strong indication for development of a CDW order in this organic superconductor. The importance of the interlayer effects in the $\kappa-(\mathrm{ET})_2\mathrm{X}$ family of organic superconductors with $\mathrm{X} = \mathrm{I}_3, \mathrm{Cu}(\mathrm{NCS})_2, \mathrm{Cu}[\mathrm{N}(\mathrm{NC})_2]\mathrm{B}_\mathrm{r}$ has been discussed in Ref. [38] as a common feature in these materials. Thermal-expansion measurements have shown that in all three materials there are pronounced negative effects at the transition temperature T_c for stress parallel to the conducting planes. Concerning the second dip in the magnetothermopower of $\kappa-(\mathrm{ET})_2\mathrm{Cu}(\mathrm{NCS})_2$ around the magnetic breakdown field it might also be associated to the interlayer effects. This can be correlated with the dominant presence of the $\beta-\alpha$ frequency in the magnetothermopower FFT spectrum in the high field region which is found to have similar effective mass as the fundamental α frequency which is dominant frequency in the low field region. Our suggestion is that, in the organic superconductor $\kappa-(\mathrm{ET})_2\mathrm{Cu}(\mathrm{NCS})_2$, the two transitions that appear at low and high field region are realized by the same mechanism, implying that they consist of two similarly ordered states.

4. CONCLUSIONS

The interlayer magnetothermopower of the organic superconductor $\kappa-(\mathrm{ET})_2$ $\mathrm{Cu(NCS)}_2$, in the direction perpendicular to the layers, is found to drop with decreasing temperature T and becomes negative, a behavior similar to that observed in the Seebeck effect in the high-T_c cuprate YBCO. Another common feature is the presence of a dip leading to an upturn in the magnetothermopower at low fields. Moreover, in $\kappa-(\mathrm{ET})_2\mathrm{Cu(NCS)}_2$ a second dip appears in the high field region leading to a smaller upturn which has not been observed in YBCO. The first dip is seen at a magnetic field of 7 T slightly above the upper critical field and the second one is around the magnetic breakdown field. We correlate the presence of the dip feature with the existence of CDW modulations along the interlayer direction in this superconductor. We ascribe the possible CDW order in $\kappa-(\mathrm{ET})_2\mathrm{Cu(NCS)}_2$ to the interlayer effects, *i.e.*, to the layer-stacking mechanism rather than to the nesting instabilities. We find that the magnetothermopower oscillation amplitude deviates from the LK behavior at fields below 10 T and temperature above 1 K but is well described if we take into account the thermodynamic layer-stacking in this material. We suggest that the two dips observed in the magnetothermopower of $\kappa-(\mathrm{ET})_2\mathrm{Cu(NCS)}_2$, in the normal state, describe two induced phase transitions in both low and high field region that correspond to two similarly ordered states driven by the same mechanism.

Acknowledgements. The work was performed at the National High Magnetic Field Laboratory, supported by NSF DMR-0654118, by the State of Florida, and by the DOE.

REFERENCES

1. K. Kanoda, Physica C **282-287**, 299 (1997).
2. R. McKenzie, Science **278**, 820 (1997).
3. T. Sasaki, H. Sato, and N. Toyota, Solid State Commun. **76**, 507 (1990).
4. T. Sasaki, H. Sato, and N. Toyota, Physica C **185-189**, 2687 (1991).
5. J. Caulfield, W. Lubczynski, F.L. Pratt, J. Singleton, D.Y.K. Ko, W. Hayes, M. Kurmoo, and P. Day, J. Phys.: Condens. Matter **6**, 2911 (1994).
6. K. Oshima, H. Urayama, H. Yamochi, and G. Saito, Physica C **153-155**, 1148 (1988).
7. T. Sasaki, W. Biberacher, K. Neumaier, W. Hehn, K. Andres, and T. Fukase, Phys. Rev. B **57**, 10889 (1998).
8. M. M. Mola, S. Hill, J. S. Brooks, and J. S. Qualls, Phys. Rev. Lett. **86**, 2130 (2001).
9. T. Sasaki, T. Fukuda, T. Nishizaki, T. Fujita, N. Yoneyama, N. Kobayashi, and W. Biberacher, Phys. Rev. B **66**, 224513 (2002).
10. V. M. Gvozdikov, Yu. V. Pershin, E. Steep, A. G. M. Jansen, and P. Wyder, Phys. Rev. B **65**, 165102 (2002).
11. T. Sasaki, T. Fukuda, N. Yoneyama, and N. Kobayashi, Phys. Rev. B **67**, 144521 (2003).
12. J. Schmalian, Phys. Rev. Lett. **81**, 4232 (1998).
13. K. Izawa, H. Yamaguchi, T. Sasaki, and Y. Matsuda, Phys. Rev. Lett. **88**, 027002 (2002).

14. T. Arai, K. Ichimura, K. Nomura, S. Takasaki, J. Yamada, S. Nakatsuji, and H. Anzai, Phys. Rev. B **63**, 104518 (2001).
15. D.J. Scalapino, E. Loh, Jr. and J.E. Hirsch, Phys. Rev. B **35**, 6694 (1987).
16. J. Merino and R. H. McKenzie, Phys. Rev. Lett. **87**, 237002 (2001).
17. M.V. Kartsovnik, A.E. Kovalev, and N.D. Kushch, J. Physique I **3**, 1187 (1993).
18. E. S. Choi, J. S. Brooks, J. S. Qualls, and Y. S. Song, Rev. Sci. Instrum. **72**, 2392 (2001).
19. O. Cyr-Choinire, S. Badoux, G. Grissonnanche, B. Michon, S.A.A. Afshar, S. Fortier, D. LeBoeuf, D. Graf, J. Day, D.A. Bonn, W.N. Hardy, R. Liang, N. Doiron-Leyraud, and L. Taillefer, Phys. Rev. X **7**, 031042 (2017).
20. T. Sasaki, N. Yoneyama, A. Matsuyama, and N. Kobayashi, Phys. Rev. B **65**, 060505(R) (2002).
21. E.S. Choi, J.S. Brooks, and J.S. Qualls, Phys. Rev. B **65**, 205119 (2002).
22. D. Krstovska, E. Steven, E.S. Choi, and J.S. Brooks, Low Temp. Phys. **37**, 950 (2011).
23. F.L. Pratt, J. Caulfield, L. Cowey, J. Singleton, M. Doporto, W. Hayes, J.A.A.J. Perenboom, M. Kurmoo, and P. Day, Synth. Metals **55-57**, 2289 (1993).
24. H. Ito, T. Ishiguro, T. Komatsu, G. Saito, and H. Anzai, Phisica B **201**, 470 (1994).
25. S. Friemel, C. Pasquier, and D. Jerome, Physica C **292**, 273 (1997).
26. F. Zuo, J. A. Schlueter, M. E. Kelly, and J. M. Williams, Phys. Rev. B **54**, 11973 (1996).
27. M.V. Kartsovnik, G. Yu. Logvenov, K. Maki, and N. D. Kushch, Synth. Metals **103**, 1827 (1999).
28. J. Singleton, J. A. Symington, M.-S Nam, A. Ardavan, M. Kurmoo, and P. Day, J. Phys.: Condens. Matter **12**, L641 (2000).
29. N. Harrison, J. Caulfield, J. Singleton, P. H. P. Reinders, F. Herlach, W. Hayes, M. Kurmoo, and P. Day, J.Phys.: Condens. Matter **8**, 5415 (1996).
30. M.-S. Nam, M. M. Honold, C. Proust, N. Harrison, C. H. Mielke, S. J. Blundell, J. Singleton, W. Hayes, M. Kurmoo, and P. Day, Synth. Met. **103**, 1905 (1999).
31. T. Maniv, V. Zhuravlev, I. Vagner, and P. Wyder, Rev. Mod. Phys. **73**, 867 (2001).
32. H. Ito, S. M. Hayden, P. J. Meeson, M. Springford, and G. Saito, J. Supercond. **12**, 525 (1999).
33. N. J. Clayton, H. Ito, S. M. Hayden, P. J. Meeson, M. Springford, and G. Saito, Phys. Rev. B **65**, 064515 (2002).
34. V.M. Gvozdikov, Low Temp. Phys. **27**, 704 (2001).
35. V.M. Gvozdikov, Phys. Rev. B **70**, 085113 (2004).
36. V.M. Gvozdikov, Phys. Rev. B **72**, 075135 (2005).
37. V.M. Gvozdikov, Low Temp. Phys. **37**, 1209 (2011).
38. J. Müller, M. Lang, J. A. Schlueter, U. Geiser, and D. Schweitzer, Synth. Met. **120**, 855 (2001).